nature portfolio

Peer Review File

Large seafloor rupture caused by the 1956 Amorgos tsunamigenic earthquake, Greece

Corresponding Author: Dr Frédérique Leclerc

This file contains all editorial decision letters in order by version, followed by all author rebuttals in order by version.

Attachments originally included by the reviewers as part of their assessment can be found at the end of this file.

Version 0:

Decision Letter:

** Please ensure you delete the link to your author home page in this e-mail if you wish to forward it to your coauthors **

Dear Dr Leclerc,

Please allow us to apologise for the delay in sending a decision on your manuscript titled "The discovery of the large seafloor rupture of the 1956 Amorgos tsunamigenic earthquake (Greece)". It has now been seen by our reviewers, whose comments appear below. In light of their advice we are delighted to say that we are happy, in principle, to publish a suitably revised version in Communications Earth & Environment, provided you present clarification or additional detail on the description of fault-related features, cross-cutting relationships, and follow the requested improvements on figures and wording.

We therefore invite you to revise your paper to address the remaining concerns of our reviewers. At the same time we ask that you edit your manuscript to comply with our format requirements and to maximise the accessibility and therefore the impact of your work.

EDITORIAL REQUESTS:

Please review our specific editorial comments and requests regarding your manuscript in the attached "Editorial Requests Table".

*****Please take care to match our formatting and policy requirements. We will check revised manuscript and return manuscripts that do not comply. Such requests will lead to delays. *****

Please outline your response to each request in the right hand column. Please upload the completed table with your manuscript files as a Related Manuscript file.

If you have any questions or concerns about any of our requests, please do not hesitate to contact me.

SUBMISSION INFORMATION:

In order to accept your paper, we require the files listed at the end of the Editorial Requests Table; the list of required files is also available at https://www.nature.com/documents/commsj-file-checklist.pdf .

OPEN ACCESS:

Communications Earth & Environment is a fully open access journal. Articles are made freely accessible on publication. For further information about article processing charges, open access funding, and advice and support from Nature Research, please visit https://www.nature.com/commsenv/open-access

At acceptance, you will be provided with instructions for completing the open access licence agreement on behalf of all authors. This grants us the necessary permissions to publish your paper. Additionally, you will be asked to declare that all required third party permissions have been obtained, and to provide billing information in order to pay the article-processing charge (APC).

Please use the following link to submit the above items:
Link Redacted
** This url links to your confidential home page and associated information about manuscripts you may have submitted or be reviewing for us. If you wish to forward this email to co-authors, please delete the link to your homepage first **

We hope to hear from you within two weeks; please let us know if you need more time.

Best regards,

Derya Gürer, PhD
Editorial Board Member
Communications Earth & Environment
orcid.org/0000-0001-5884-9160

Joe Aslin
Deputy Editor,
Communications Earth & Environment
https://www.nature.com/commsenv/
Twitter: @CommsEarth

REVIEWERS' COMMENTS:

Reviewer #1 (Remarks to the Author):

This paper reports ROV observation of submarine fault scarp recording movements of a historic tsunami-genic earthquake. The presented data, especially ROV photos (as 3D models), are fascinating and highly suggestive for us about underwater exploration of earthquake faults. Resultant discussions are also clear and reasonable. I thus think it is worth publishing. In some parts, more detailed description is desired to make the story robust. I'll be glad if following my comments help it.

Major comments:
(1) Lines 217-219: Better to describe characteristics of subvertical striae more in detail. For example:
* Striae found on the colluvial wedge surface (Figs. 3a and S-3F) are clearly identified as sediment rills.
* In Fig. S2B, the striae on the mirror are crosscut (covered) by the top of the recent colluvial wedge at their lower end, excluding their origin from current sedimentary processes.
* In Fig. S2B, the striae seem to be covered by breccia-like materials labeled as "Block that is part of the colluvial wedge" at their upper ends. However, the wedge seems to consist of finer-grained sediments (white ooze?) as seen in the paleo-wedge in the same fig. and also in the modern wedge in Figs. S1b &c. Therefore, it is more probable that the breccia-like materials are fault breccia hanging on the mirror surface, rather than parts of the colluvial wedge. This interpretation, if correct, supports that the striae are tectoglyphs scratched by the brecciated hanging-wall materials (see the attached file).
* In Fig. S2E, striae on the fresh mirror are seemingly covered with remnants of the paleo-wedge. This relation implies that the striae formed not in the last event but in previous events before the paleo-wedge formed (even though the mirror surface appeared in the last event). This also implies that not paleo-wedge sediments but deeper portions of the hanging-wall scratched the mirror surface to form the striation.
No matter whether the authors agree or disagree with arguments above, more detailed description especially on crosscut relations could better constrain the origin and timing of the observed features.

(2) Each picture in Figs. 3 and S2 is a computed collage of multiple photographs. In each source photograph (or a snapshot of 4K video), brightness might reflect not only color of pictured materials (rock or sediment surfaces), but also lighting: brighter parts are closer to, and darker parts are farther from the ROV LED lights. Such lighting effects seem to be not fully corrected to create 3D collages, resulting in artificially mottled appearance of the presented pictures. This could be a problem for the story: I wonder whether the upper darker parts in Figs. 3 and S2B–G owe really to Mn coating or merely to poor lightning. Because ROV did not go upslope so much (as shown in Fig. 2), the top parts of the observed slopes might have been always remote from the vehicle and thus pictured as dark. One of the ways to cancel this discrepancy may be showing raw pictures for key features. Although 3D models appear attractive, they are not observation (in strict sense) but artificially processed models. I recommend also to show raw pictures as primary data.

(3) Estimation of fault displacement relies on identification of remnants of the last colluvial wedge hanging on the scarp. Therefore, it is better to more clearly describe that there are no other remnants at lower levels than the observed remnants identified as the last. In Fig. S2F, there seems to exist potential another remnant at a lower level than that labeled as paleo-wedge. It is desired to have explanation on what is this. In addition, there might be no proof that remnants of the paleo-wedge are always preserved on the upheaved mirror surface. If the paleo-wedge happened to be unpreserved in a place,

the second last could be identified as the last. Such misidentification, if happens, overestimates the fault displacement. Although the authors' identification feels acceptable because all lie at similar levels, I feel it still better to briefly describe such theoretical limit or assumption before evaluation of displacements.

Minor comments:
(4) Better to provide geological background more in detail. What kind of rocks comprise the fault scarp? Are they hard or soft? Even if ROV observation could not specify the exact rock species, citing literature on underwater geology such as dredge reports could be useful. Nature of bed rocks are important for readers to properly understand implication of the observed features.

(5) Line 180: “At one place”: Better to describe precise location (lat & lon etc.).

(6) Line 217 and Fig. 3: The parts indicated as gouge in Fig. 3 looks like covers rather than gouge. The parts are so smooth and fine-grained, whereas gouges usually consist of fractured particles of heterogeneous grain sizes. Because it has passed nearly 70 years, it is natural that the mirror surface is partly blanketed with recent mud. Anyway, it's better to describe the reason why a feature was identified as so.

(7) Is there any published data on ages of ancient tsunami deposits around the study area? If present, they could support the discussion in lines 314–321 on recurrence interval of the tsunami-genic earthquakes.

(8) Fig.2: Although 3D view is somewhat reader-friendly, such a bird's-eye-view cannot show features (slope angle, dimension, etc.) accurately. A plain view topo map, which expresses much more delicate features, has been provided as Fig. S1a. In addition, if topographic cross sections are also shown, readers can more accurately understand the slope characteristics.

(9) Fig.3: Please clarify whether panels b–e are close-up views of the same 3D model as the panel a or raw pictures.

Reviewer #2 (Remarks to the Author):

This is a very well-written and interesting paper that should be of great interest to a wide range of earthquake and tsunami scientists, as well as marine geologists. It describes a study that identifies the source of an import tsunamigenic earthquake in the Mediterranean Sea in 1956. In some cases it is possible to guess with reasonable confidence which submarine fault ruptured to generate a major historic tsunami, there are many cases the source remains enigmatic (like the 1755 Lisbon tsunami). Even for modern tsunamis, the precise mechanism for generation - fault rupture or earthquake-triggered submarine landslide? - is often pootly understood - like the case of the 2018 Paul tsunami. This paper gives what appears to me to be the most compelling case ever for identification of fault rupture that generated a tsunami based on marine geologic evidence. I think its conclusions are supported by the data, and that it represents an important step forward in the study of tsunami sources.
I think that the paper could be published in essentially its present form, although I have a few minor suggested changes as indicated below.

1) I was confused by the description of how the “shifted” GPS velocities in Fig. 1 highlight the “stability” of the central Aegean, and wonder if the figure and wording could be improved. There should be a velocity scale for the purple GPS vectors and the reference frame for the velocity determinations should be stated. Are these with respect to the Aegean Sea or the Eurasian Plate? Which sites do the 15.6 mm/yr east and -25 mm/yr north velocities refer to (obviously both sites have both east and north components), and why do these differ from the 4 mm/yr “relative displacement” (is it not a velocity?, and relative to what?).
In any case velocities which differ from that associated with rigid block motion either reflect deformation do to friction at plate boundaries that experience relative movement, or the presence of additional mcrooplates, or both. I would say they highlight complex tectonics rather than stability.

2) On Line 162, I think it would be worth having a sentence or two to explain what a “fault mirror” is, and what its significance is

Line 56: “hypocenter” -> “hypocentral depth”
Line 97: “entered” -> “inundated”
Line 104: “inducing” -> “so”
Line 116: “archeological masonries” -> “damage to archaeological masonry structures”
Line 263: “is no testimonies”” -> “are no testimonies”

Reviewer #3 (Remarks to the Author):

Dear Authors,

It is with a great interest that I read your manuscript entitled:"The discovery of the large seafloor rupture of the 1956 Amorgos

tsunamigenic 1 earthquake (Greece)" co authored by Leclerc F., Palagonia S., Feuillet N., Nomikou P., Lampridou D., Barrière P., Dano A., Ochoa E., Gracias N. and Escartin J.
With your new observations you evidence for the first time a recent seafloor rupture along the active fault of Amorgos (Greece), that may have trigger the tsunami that followed the Amorgos 1956 earthquake, challenging the hypothesis of a landslide as a source for the observed tsunami.
Your study open a new avenue to the study of monitoring large active faults located next to populated area such as islands along subduction zones worldwide. Such systematic studies might allow a better risk assessement and would be benefic for policy makers.
I thus recommend the editor to accept your mansucript with very minor revisions mostly concerning the figures (see my comments in the annotated manuscript).
Best regards

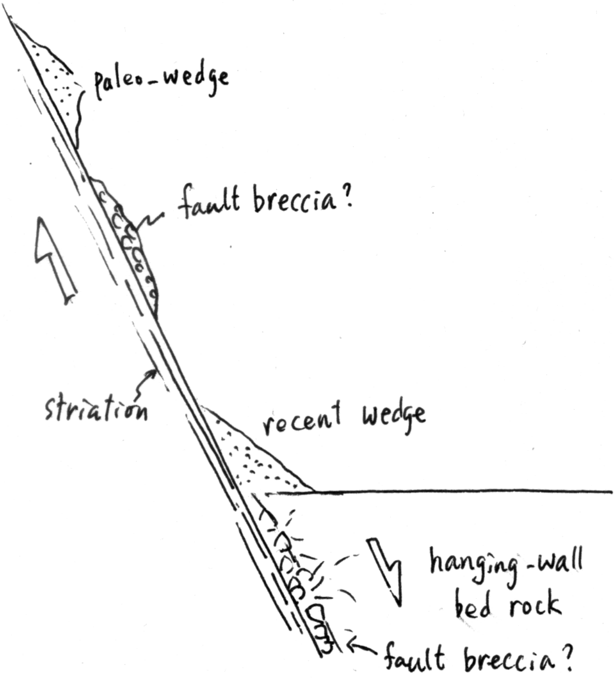

paleo-wedge
fault breccia?
striation
recent wedge
hanging-wall
bed rock
fault breccia?

The discovery of the large seafloor rupture of the 1956 Amorgos tsunamigenic earthquake (Greece)

Leclerc F.[1*], Palagonia S.[1], Feuillet N.[2], Nomikou P.[3], Lampridou D.[3], Barrière P.[1], Dano A. [1], Ochoa E. [4], Gracias N.[4], Escartin J.[5]

1- Université Côte d'Azur, CNRS, Observatoire de la Côte d'Azur, IRD, Géoazur, 250 rue Albert Einstein, Sophia Antipolis 06560 Valbonne, France.
2- Université Paris Cité, Institut de Physique du Globe de Paris, CNRS, F-75005, Paris, France
3- Department of Geology and Geoenvironment, National and Kapodistrian University of Athens, Panepistimioupoli Zografou, Athens, 15784, Greece
4- Computer Vision and Robotics Institute, University of Girona, Girona, Spain
5- Laboratoire de Géologie, Ecole Normale Supérieure (CNRS UMR 8538), PSL Research University, Paris, France

** Corresponding author : leclerc@geoazur.unice.fr

In recent decades, large offshore earthquakes have proven dangerous, capable of triggering tsunamis along densely populated and economically significant coastlines. In the Mediterranean Sea, the probability that a large earthquake-triggered tsunami will occur in the next few decades is high[1]. European tsunami databases[2] document the geographical occurrence of historical and modern tsunamis. However, we often lack information about the tsunami sources, preventing us from assessing the hazard properly[3]. In particular, the faults that slipped during earthquakes and displaced the

seafloor to generate tsunamis, often remain unidentified. Here we identify the submarine rupture of the Amorgos earthquake that on July 9, 1956, triggered the largest tsunami[4,5] in the Mediterranean Sea in the past two centuries, demonstrating that tsunami sources can be determined several decades after the event. Using submarine vehicles, we explored all the major normal faults offshore Amorgos and Santorini islands. We discovered a large surface rupture along the 75-km long Amorgos fault, presenting markers of slip, still visible six decades after the earthquake. The large seafloor offset identified ranges between 9.8 and 16.8 m, compatible with a Mw 7.5 event. This finding prompts a reassessment of the origin of the largest tsunami waves (≥20 m), previously attributed to earthquake-triggered submarine mass-wasting.

Surface ruptures generated by large continental earthquakes, whether historical[6,7] or recent[8], are today systematically mapped through fieldwork, satellite data and high resolution topographic analyses. They provide key information that allows the seismic hazard of a region to be evaluated, in particular through identification of the causative fault, the extent of the rupture, and the amount of slip generated by the earthquake. Such work was performed in only a few weeks following the 2023 Turkey-Syria earthquake[9] for example. When the earthquake occurs offshore, similar analyses are challenging to perform, but they are of prime importance to understand the triggering of tsunamis and evaluate the seismic hazard along submarine faults. The recent deployment of submarine vehicles (such as Remotely Operated Vehicles ROVs), however, offers new opportunities to image undersea fault scarps[10,11,12,13], identify fault planes that have been recently exhumed by slip during an earthquake[14], and map and quantify the related surface rupture[15]. With such a vehicle, we investigated the faults around the proposed epicenter of the 1956 Amorgos earthquake to identify seafloor ruptures and determine the fault responsible for this event.

The 1956 earthquake and tsunami

The Amorgos earthquake occurred on July 9, 1956, offshore Santorini and Amorgos (Cyclades, South Aegean Sea), along the Hellenic Volcanic Arc. It was recorded by a small number of seismometers, enabling seismologists to determine a magnitude of 7.2 to 7.8[16], depending on the authors. Several epicenters were obtained[17] that locate the earthquake between 5 and 20 km south of Amorgos island (Figure 1). Its hypocenter, recognized to be poorly constrained[5] and debated[18], varies between 10 km and 45 km, and was recently re-evaluated at ~25 km[17], that is, at the Moho depth of the Hellenic arc[19]. The main shock was followed by a series of aftershocks. The first aftershock, called the twin earthquake, had a magnitude estimated between 6.0 and 7.2, and occurred only 13 minutes later, closer to Santorini (Figure 1) and probably deeper (40-95 km), possibly along the subduction plate boundary[17]. The main shock caused severe damage on the surrounding islands, subsequently enhanced by the twin shock, especially in Santorini[20]. More than 3200 buildings were damaged, including ~500 that were completely destroyed; in addition, 54 people were killed in Santorini and 100 people were injured.

Several focal mechanisms were obtained to characterize the faults that are likely to have broken. The best constrained ones point to a NE-SW striking normal fault plane[17,5], in agreement with the local tectonic context and secondary faults visible along the southern coast of the island[20,21,22] (Figure 1). The coseismic slip probably occurred on a SE-dipping plane, calculated to be either a low-dipping plane (25°)[5] or a steeper dipping plane (~65°)[17] (both shown in Figure 1), the latter being more typical of a normal fault. However, our knowledge of the fault that broke and produced this earthquake has until now been incomplete, due to our inability to identify and map the undersea fault.

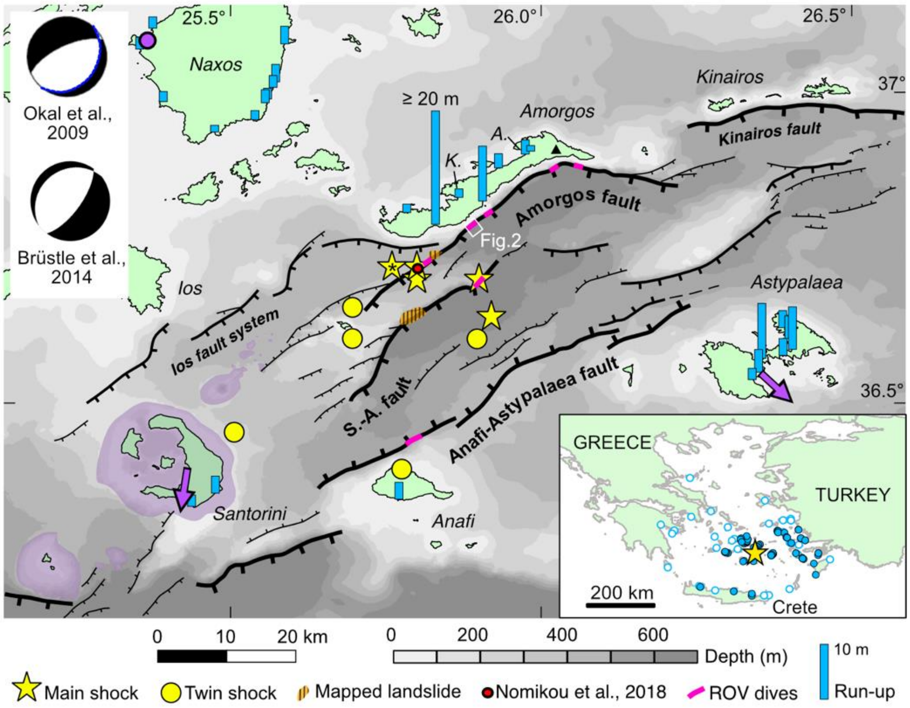

Figure 1: Seismotectonic map in the epicentral area of the July 9th, 1956 earthquake. *Several epicenters for the main shock (star) and twin shock (dot) are represented, as summarized in Brüstle et al. (2014)[17], with two proposed focal mechanism[17,5] calculated for the epicenter marked with a star and an asterisk. Main faults are represented by black lines, with thicker traces for longer and taller faults, and are modified from previous works[22,30,34]. S.-A. fault: Santorini-Amorgos fault. Portions of faults explored with the ROVs during the AMORGOS-23 cruise are in pink. Submarine landslides identified[26] are in dashed orange, while the observation[22] of a probable fault mirror associated with the 1956 event along the Amorgos fault is a red dot. Measured run-ups[5] are represented as blue bars. In the inset, tsunami observations are located by blue[5] and white[4] dots. Light purple areas are onshore and offshore volcanoes. The purple arrows on Santorini and Astypalaea and the purple dot on Naxos show GPS velocities that have been shifted by 15.6 mm/yr east and −25.2 mm/yr north with respect to the velocity of stable Europe[32]. These highlight the stability of the central Aegean (Naxos) and the ~4 mm/yr relative displacement of Astypalae and Santorini toward the southeast and southwest, respectively. Mount Kroukelos on Amorgos is denoted by a black triangle. The two*

archeological sites that demonstrate long-term subsidence of the northern coast of Amorgos[21] are located in Katapola (K.) and Aegiali (A.).

In addition, the main shock triggered a large tsunami that reached the coastlines of Crete, Peloponnesus, western Turkey[4,5,23], and that was recorded by one tide gauge in Israël[24]. Amorgians today still recall that after the earthquake, the sea retreated, allowing pedestrians to cross the Katapola bay, before it entered the land, with waves of 2-3 m high (Figure 1). Along the southern coast of Amorgos island, run-ups of up to 20 m were reported[4,5] while the northern coastline of Astypalaea island was also flooded with run-up of up to 10 m[4,5,25] (Figure 1). These values are the highest reported in the Mediterranean basin in the twentieth and twenty-first centuries[2]. Despite a re-assessment of the testimonies made of this tsunami[5], the details of the arrival time of the wave remained vague[5] across the archipelago, as remains our knowledge of the first wave polarity[23]. Tide gauges installed in Crete and in Leros were damaged by the earthquake, inducing that the tsunami arrival was not recorded[23] in the near-field.

To explain the variation and local tsunami run-up heights along the coasts, a second source of sudden submarine seafloor motion was proposed, in addition to slip on a low-angle normal fault[5]. Waves were probably enhanced by submarine landsliding[4], later observed at the seafloor[26] in the archipelago (Figure 1). Such a scenario was tested with tsunami modeling[5,24] that aimed at reproducing tsunami data (run-ups only[5]), using pre-determined source geometries. The geometry of the basins and the coastal bathymetry that greatly influence the run-up values at the coasts[27] were, and are mostly still, unknown, and thus un-used in tsunami modeling[5]. All in all, the primary source of the earthquake and tsunami remains debated[28], as epicentral solutions, tsunami data and coastal bathymetric data are not sufficiently constrained.

On-land investigations were conducted to gain new insights into the origin of the events. On Amorgos island, uplifted and subsided shorelines, as well as archeological masonries (Figure 1), suggest the break of a steep normal fault located within 5 km of the Amorgos' southern coast[21]. Conversely, far-field subsidence of Holocene shorelines[29] are compatible with the co- and post-seismic motion generated by a deep and low-angle normal fault. Using the different markers visible on land and in coastal areas is clearly insufficient to understand this earthquake and tsunami, as they do not converge towards a common source.

The submarine faults offshore Amorgos

In the past 10 years, marine geophysical data were acquired[22,26,30,31] with sufficient resolution to identify, map and characterize the faults in the area (Figure 1). A 750-m deep, NE-SW striking trough, measuring 35 km in width, exists between the islands of Ios, Amorgos and Kinairos to the north, and Anafi and Astypalaea to the south. This trough is bordered to the north by a set of NE-SW to E-W striking normal faults, dipping to the south-southeast.

The main fault is the Amorgos fault, which constitutes the southern cliff of Amorgos island, whose summit reaches 821 m (Mt Kroukelos, Figure 1). The main segment of the fault measures 45 km (Figure 1, thick dark line), and up to 75 km if we consider secondary structures that connect or align with the main fault at its tips (Figure 1, thin dark lines). Its activity induces the subsidence of its hanging wall, marked by the depth of Amorgos basin, reaching ~ 750 m below sea level[22,30]. Seismic reflection profiles acquired in the basin reveal that 700 meters of sediments, tilted to the north, that is, toward the fault, cover the alpine basement[22], indicating about 2.2 km of vertical offset by the Amorgos fault.

The southern border of the trough is structured by the NE-SW striking, NW-dipping Anafi-Astypalaea fault system that extends from NW of Anafi to NW of Astypalaea island (Figure 1). This fault is segmented and in its central part it presents several sub-parallel smaller faults offsetting its hanging wall[30]. Its cumulative offset is significantly lower than that of the Amorgos fault, about 1 km in its western part[31], and it measures about 65 km in length.

In between the two main antithetic faults, several other faults offset the seafloor, creating horsts and grabens, including the Santorini-Amorgos (S-A) fault, located at ~8 km from the southern coasts of Amorgos. This structure is a NE-SW striking, SE-dipping normal fault, offsetting the basement by about 1.1 km[22]. In total, the Santorini-Amorgos fault measures about 55 km.

The orientation of this fault system is compatible with the two nodal planes of the focal mechanisms of the 1956 earthquake (Figure 1). At the scale of the trough, these faults thus seem to accommodate mainly a NW-SE extension, in line with recent GPS data showing a NW-SE-oriented velocity gradient of 4 mm/yr between Naxos and Astypalea[32] (Figure 1). On a larger scale, this fault system might accommodate some lateral motion of the southern Aegean domain with respect to the central Aegean domain, but this is still debated[30,32,33,34].

Considering the uncertainty of the earthquake location and the incompleteness of the tsunami data, the three main faults of this system, that is, the Amorgos, Santorini-Amorgos, and Anafi faults, are all good candidates as sources for the 1956 main shock (Figure 1). Moreover, as the surface (and thus length) of a fault is proportional to the magnitude of the largest earthquake it can generate[35,36], the three faults are all long enough to host an $M \geq 7$ earthquake such as the Amorgos 1956 main shock. However, recently acquired seismic reflection profiles[22] imaged a particularly steep 8-10 m high scarp at the base of the Amorgos fault (Figure 1). This suggests that a recently exhumed fault mirror may be preserved here, and thus that this fault could be the source of the 1956 earthquake.

We surveyed the three faults for the first time using an Autonomous Underwater Vehicle (AUV) and a Hybrid Remotely Operated Vehicle (HROV) onboard the R/V Europe[37,38], in order to characterize the faults' morphologies with bathymetric data (resolutions of 1 and 10 m), and image its surface to identify potential ruptures using 4K optical imagery (Figure 1). The strategy carried out to survey optically each of the three faults was the same : HROV dives were performed close to the epicentral area, and at places where the cumulative scarps are the steepest (identified in the bathymetry) and the simplest (deformation is accommodated along one fault scarp only, observations were made far from fault relays). Dives are performed away from large mass-wasting scars and deposits that could have erased and buried the markers of surface rupture on the seafloor. With this strategy, we identified that the Amorgos fault is the only one to exhibit a freshly exhumed fault mirror at the base of its cumulated scarp (Figure 2, 3).

A fault mirror with fresh exhumation traces

Offshore the south-eastern coast of Amorgos island, the new high-resolution bathymetric data reveals that the Amorgos fault exhibits a >600 m high submarine scarp visible all along its strike. At one place shown here, this scarp is particularly steep (60°) and linear (Figure 2a). It shows neither segmentation nor synthetic or antithetic parallel splays, inducing that the deformation localizes here along a single fault plane.

In the 1-m resolution Digital Elevation Model (DEM), the base of the cumulative scarp is smooth, showing only a few narrow gullies, parallel to the slope, that incise it (Figure 2a). At the gullies' outlet, small cones are visible and cover locally the fault scarp. The base of the fault scarp dips between 35° and 60° (Figure 2 a,c), a range comparable to the dips determined at depth with geophysical[22] and seismological[28] observations (38°-66°). A colluvial wedge covers its foot, and dips toward the basin, with slopes up to 30° close to the scarp, and only 2° at 300 m far from the scarp (Figure 2a).

Close to the scarp, the colluvial wedge has been locally eroded by failures and gravity collapses, and shows local depressions that are up to two meters deep (Figure 2a, b). HROV optical images allow analyzing the cliffs around the depressions that expose the sediment strata constituting the wedge (Figure S1). They are ~1 m thick strata, composed of fine sediment, and dip toward the basin (away from the fault). Bedding might have played the role of decollement, facilitating slope-failure within the colluvial wedge.

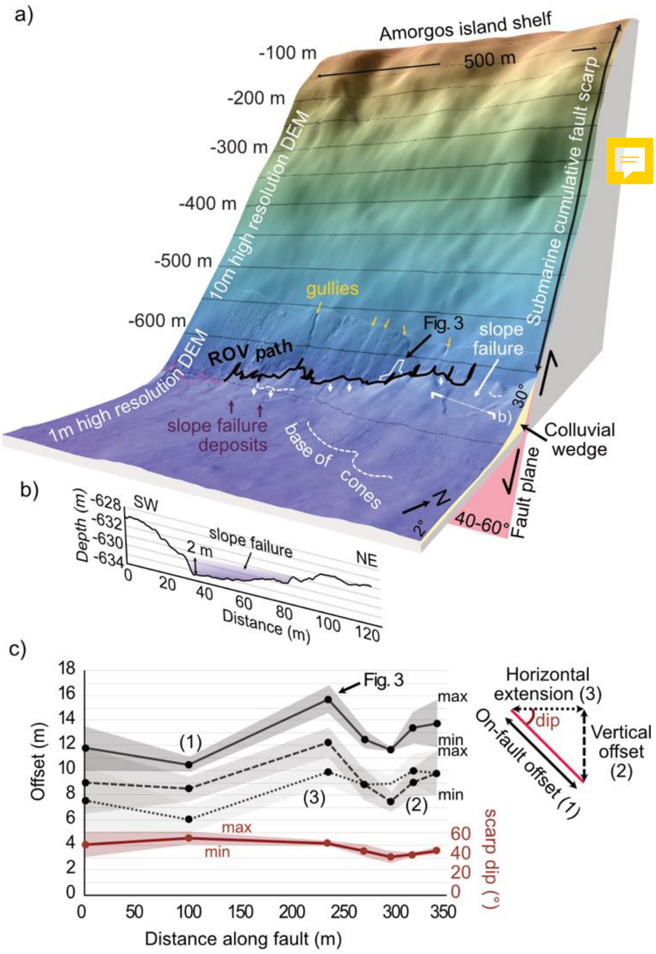

Figure 2: a) 3D view of the morphology of the submarine Amorgos fault. *A 500m long portion of the fault (located in Figure 1) is represented in 3D with no vertical exaggeration. The HROV investigated the base of the fault scarp (navigation in pink and black). Gullies (yellow arrows) incise the fault mirror. At their outlets, cones of sediments (dashed white lines) are visible, they*

are affected by slope failures (white arrows) that deposit in the deep basin. b) Bathymetric profile across one slope failure allow determining that it is at most 2 m deep (b - purple area). c) On-fault offsets of the seafloor (1) measured on digital outcrop models (DOMs) of the fault mirror, acquired along several vertical transects (corresponding to the black ROV path on a) are shown by dots linked by a solid line. The upper bound of the grey surface associated to the line corresponds to the maximum on-fault offsets measured on the DOMs, while the lower bound corresponds the minimum. One DOM presented in Figure 3 is located on both a) and c). The fault mirror dip (in red) and its variations (red surface bounded by minimum and maximum dips) were measured in the 1 m DEM, allowing us to calculate the corresponding vertical offsets (2) and horizontal extensions (3) (and their uncertainties shown as grey surfaces).

Using the 4K camera of the HROV Ariane, we identified a smooth and well preserved fault mirror at the base of the cumulative scarp (Figure 3, S2), over a length of ~750 m. At some places, the fault mirror exhibits gouge coatings and also striae that are sub-vertical (Figure 3d, e). We interpret the latter as tectoglyphs due to a dip-slip fault motion, but the shapes of some of them are probably accentuated by sediment-sliding down the fault plane, forming rills. The fault mirror also exhibits a light brown color surface over the first ~10 m or more, while above the scarp is often covered by a dark coating (Figure 3a, b, c, S2), or has a rougher aspect (Figure S4). Such color and roughness changes are often observed at seismically active faults on land[39,40], and are an indicator of surface ageing due to weathering of different portions of the fault that have been exhumed at different periods, due to seismic displacement. The color changes we observe on the Amorgos fault are also characteristic of active submarine faults[14,15], with coatings of Fe-Mn oxide, depositing at very slow rates (1 μm/yr to 0.125 mm/yr[41]) but efficiently darkening surfaces exposed to seawater. Lighter fault sections have thus been recently exposed.

Furthermore, in some places, the fault mirror is also topped by a thick stripe of fine white sediment (Figure 3a, b, c, S2), that is undistinguishable in appearance from the hemipelagic sediment of the wedge below, seen within failure scars (Figure S1). We interpret this deposit as being the top of the sediment wedge abutting the fault scarp prior to the earthquake, that has been detached from the hanging wall (i.e., the sediment wedge, Fig. 3f, g) by relative subsidence with respect to the footwall (i.e., the fault scarp). Similar tectonically uplifted remnants of soil[42] or colluvial wedge[43] are exhumed and uplifted by coseismic fault slip on land.

Georeferenced and scaled digital outcrop models (DOMs) of seven vertical transects have been calculated from the HROV 4K videos (Figure 3, S2). DOMs allow quantifying the offset of the seafloor by measuring the distance between the present contact of the scarp and colluvial wedge, and the paleo-contact that is now uplifted. This paleo-contact is identified either by the top of the paleo-wedge or by a color change. We measured the distance in the direction of the sub-vertical striae, along the fault plane (along-dip). In the seven sites, this on-fault distance ranges between 9.8 and 16.8 m (Figure 2-c, Table S3). We attribute this variability over the ROV path to local erosion and sedimentation processes (in the form of small failure depressions and small cones, Figure 3-a) that affect the current colluvial wedge since the fault slip. Small-scale variations in the strike, dip and rake of the fault certainly generate a variability in the measured vertical offset[44], but not to the extent observed along these ~500 m of fault. Overall, the Amorgos fault exhibits a fresh fault mirror, with a mean height of 12.7 m along-dip, at the location presented here. Similar markers of recent deformation are visible at other places over ~30 km along the fault (Figure 1), but they are distributed along several fault branches, hindering offset estimation.

The preserved remnants of the paleo-wedge and the color difference on the fault scarp argue that the fault exhumation is recent. No methods exist yet that would allow sampling and dating this fault scarp. Therefore, we must look for seismic events reported in instrumental and historical catalogs[45,46,47,48,49] in order to discuss its age. Since 1956, there is no significant earthquake that occurred near the Amorgos fault[28]. Before 1956, a few historical earthquakes, not linked to volcanic activity, have struck the island of Amorgos, on December 23rd, 1733 and on April 7th, 1891 and were felt with large intensities within the archipelago. Although the location of these events is not well constrained, the distributions of the macroseismic intensities indicate epicentral areas closer to Sifnos and Chios respectively[45,46]. Before these two events, there is no testimonies indicating that a significant earthquake occurred in the vicinity of Amorgos island during the past millennium[45,46,48], nor before[45,49].

Therefore, the recently exposed fault mirror is most plausibly linked to the 1956 sequence. Fault striaes visible on the exhumed fault plane are compatible with focal mechanisms calculated of the mainshock[17]. This fault mirror recorded either solely coseismic displacement, or both coseismic and post-seismic slip, no data exist to distinguish one from the other.

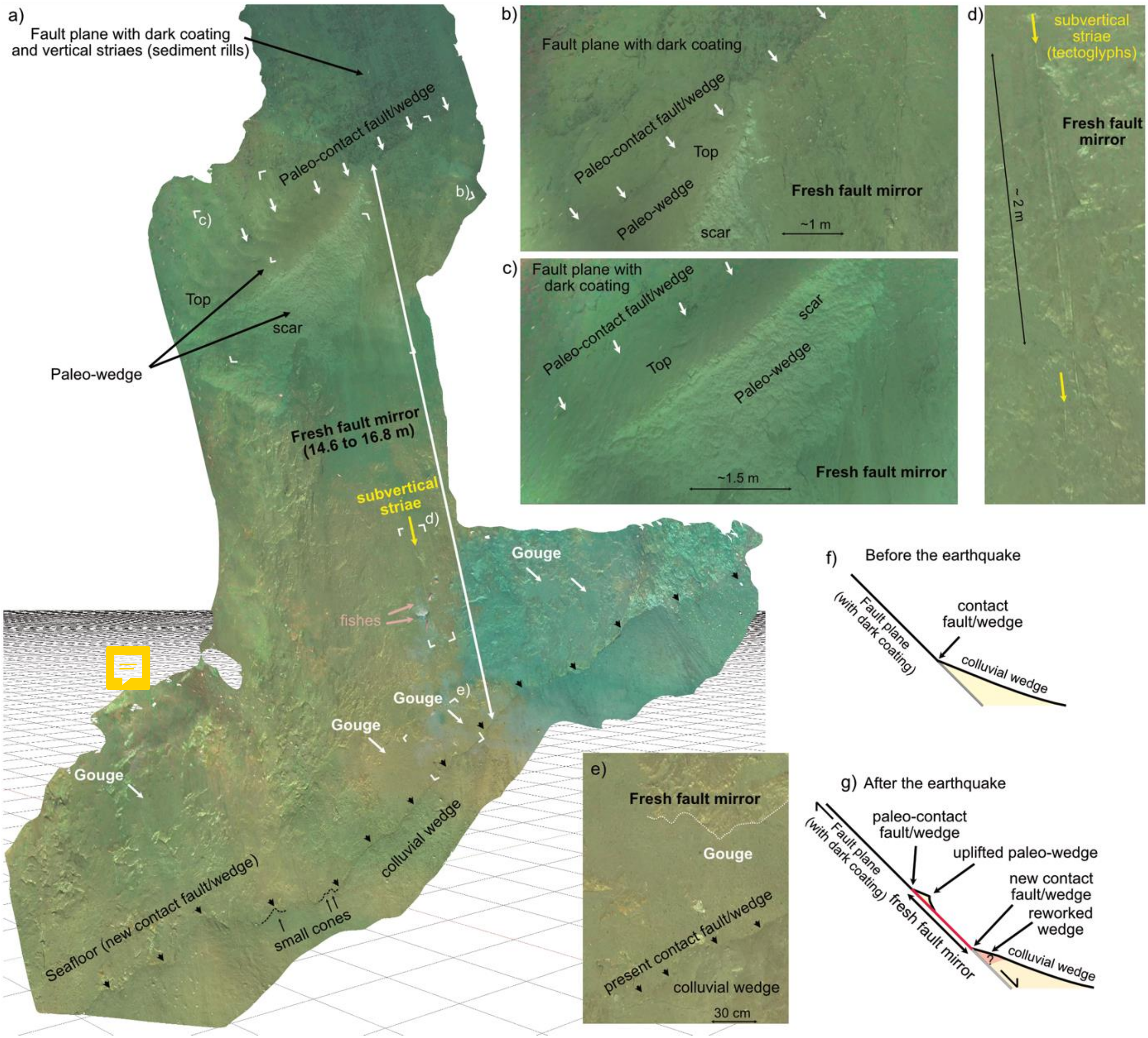

***Figure 3**: **The Amorgos fault mirror**. (a) 3D Digital Outcrop Model of the submarine fault mirror observed at the base of the Amorgos fault (location shown on Figure 2), and associated with the 1956 Amorgos event. It shows fresh tectoglyphs (d), a gouge (e), and is topped by the remnants of the paleo-wedge that has been uplifted (a, b, c). The fresh fault mirror is distinguished from the older fault plane that is darker (due to Mn coating, a, b, c). At this location, it is 14.6 to 16.8 m high (corresponding to the on-fault offset). Evolution of the fault plane morphology, before and after the earthquake, is represented by diagrams in f) and g) respectively.*

Scaling laws provide empirical correlations between earthquake magnitude and rupture parameters, including coseismic displacement, and can be used to evaluate if the displacement observed at Amorgos fault is consistent with the magnitudes of the 1956 event, or exclude it as a possible source. Even though coseismic slip is heterogeneous along a seismic rupture[50], we can tentatively calculate the seismic moment M_0 and the moment magnitude Mw of an earthquake able to generate the on-fault displacement that is observed, in order to discuss our observations. Different scaling laws link the seismic moment magnitude of an earthquake either to the rupture area A and the mean displacement on the fault[51], or to the maximum slip at the surface[52].

To use the first formulation[51], we considered that the earthquake broke the crust and reached the Moho (in agreement with the recently determined seismogenic depth[53]), along a fault dipping at 60°, with an associated rupture length ranging from 45 km (the main segment) to 75 km (the entire fault system), that the shear modulus is 3.2×10^{10} N/m^2, and that our observations correspond to the mean coseismic displacement on the fault during the earthquake. These assumptions yield a moment magnitude, Mw, ranging from 8.0 to 8.3, which is greater than the magnitude calculated from seismological data[16]. If we assume instead that the on-fault offset we observed is representative of the maximum surface displacement along the fault, the second formulation linking magnitude and maximum displacement at the surface[52] yields a moment magnitude Mw of 7.5 (±0.1), a value in line with the moment magnitude calculated with seismological data[16], which is between 7.2 and 7.8.

Seismic and tsunami hazards implications

The Amorgos tsunamigenic earthquake remains one of the largest normal faulting earthquakes recorded globally, and generated the largest tsunami in the Mediterranean Sea for the past two centuries. Our data provides the first geological evidence that the Amorgos fault was the host of this event. The Amorgos rupture identified and described in this paper shows a vertical offset that varies from 6.4 up to 13.4 m (Table S3), with a mean of about 9 m at the seafloor (Figure 2c, Table S3). This large vertical displacement, occurring only 1 km from the Amorgos coastline, suggests that the tsunami could plausibly have been triggered solely by the rupture and sudden vertical displacement of the seafloor. This justifies a revision of the role of mass-wasting in generating the highest tsunami waves, in this event, at least close to the epicentral area. While mass-wasting structures are identified in the vicinity (Figure 1), they are undated and their link to the 1956 earthquake remains to be established.

Considering the local fault dips, and the on-fault offset, the 1956 earthquake accommodated 9 m of horizontal extension on average (varying between 5 and 11.6 m, Figure 2c, Table S3). A recent study based on GNSS data[32] quantifies that the fault system between Naxos and Astypalaea must accommodate 4 mm/yr of horizontal extension. This rate implies that about 2250 years of loading is necessary to produce an earthquake similar to the 1956 main shock. If this duration represents the recurrence time for a large earthquake on the Amorgos fault, it may explain the scarcity of events in the 20th century[46, 48] and in historical records[45, 46], assuming the latter is complete. This possibility should be investigated by future paleoseismological studies in the area, in order to better constrain the seismic and tsunami hazards of the Aegean Sea and Eastern Mediterranean.

The other fault systems in the vicinity of the 1956 epicentral area, namely the Santorini-Amorgos fault, the Anafi-Astypalaea fault system, the Ios fault system and the Kinairos fault, remain unbroken today (Figure 1). Although the seismicity of the Santorini-Amorgos region is among the most sustained of the Hellenic Volcanic arc, it is largely triggered by magmatic phenomena[28] that are intense around Santorini and other submarine volcanoes (Figure 1). In historical chronicles, the closest and largest earthquake to have occurred in the vicinity of the fault system was the 42 AD event, located between Santorini and Amorgos, and was probably linked to the volcanic activity of the Santorini volcano, which erupted in 46 AD[54]. In recent times, only two Mw 6 earthquakes have occurred, in 1911 and 1919, between the Anafi-Astypalaea and Santorini-Amorgos faults[55], which are both long enough to host earthquakes of Mw $\geq$ 7. With the exception of the Santorini-Amorgos fault, the other faults left unbroken show very little microseismicity[28]. This may suggest that they are either locked and accumulating stress, or that aseismic slip is occurring[28]. The seismic coupling coefficient (SCC) calculated in this part of the Aegean Sea establishes that the region is strongly coupled (SCC ~80%)[53], except in the vicinity of Santorini (SCC~40%). This indicates that stress is mainly released in the form of large earthquakes in this region, and that the Anafi-Astypalaea fault system, the Ios fault system and the Kinairos fault could break in the future.

Sixty-seven years after the 1956 Amorgos earthquake we have used submarine vehicles to observe well-preserved and clearly visible traces of a large seafloor rupture along the Amorgos fault, allowing us to identify this as the likely source of the earthquake. This result, together with previous studies of the Les Saintes earthquake[14,15], opens the door to submarine explorations looking for the – still debated – fault sources of major historical earthquakes and tsunamis elsewhere, such as the 1783 and 1908 Messina strait events, the 1755 Lisbon earthquake and the 1833 Showa-Sanriku and 1977 Sumba outer-rise events. Comprehensive and detailed submarine geological observations will also lead to a better understanding of the mechanisms behind tsunami triggering[56]. Data from submarine exploration will be particularly important to better predict future sources of underwater earthquakes and tsunamis and to assess how our communities can adapt to these natural hazards, especially where tourism can have a major impact on a region's vulnerability.

Main References:

1-Sørensen, M.B., Spada, M., Babeyko, A., Wiemer, S. and Grünthal, G., 2012. Probabilistic tsunami hazard in the Mediterranean Sea. *Journal of Geophysical Research: Solid Earth*, *117*(B1).

2- Maramai, A., Brizuela, B. and Graziani, L., 2014. The Euro-mediterranean tsunami catalogue. *Annals of Geophysics*.

3- Grezio, A., Babeyko, A., Baptista, M.A., Behrens, J., Costa, A., Davies, G., Geist, E.L., Glimsdal, S., González, F.I., Griffin, J. and Harbitz, C.B., 2017. Probabilistic tsunami hazard analysis: multiple sources and global applications. *Reviews of Geophysics*, *55*(4), pp.1158-1198.

4 - Galanopoulos, A.G., 1957. The seismic sea wave of 9 July 1956, Prakt. Akad. Athens, 32, 90–101 (in Greek).

5- Okal, E.A., Synolakis, C.E., Uslu, B., Kalligeris, N. and Voukouvalas, E., 2009. The 1956 earthquake and tsunami in Amorgos, Greece. *Geophysical Journal International*, *178*(3), pp.1533-1554.

6- Johnson, K.L., Nissen, E. and Lajoie, L., 2018. Surface rupture morphology and vertical slip distribution of the 1959 M w 7.2 Hebgen Lake (Montana) earthquake from airborne lidar topography. *Journal of Geophysical Research: Solid Earth*, *123*(9), pp.8229-8248.

7- Haddon, E.K., Amos, C.B., Zielke, O., Jayko, A.S. and Bürgmann, R., 2016. Surface slip during large Owens Valley earthquakes. *Geochemistry, Geophysics, Geosystems*, *17*(6), pp.2239-2269.

8- Civico, R., Pucci, S., Villani, F., Pizzimenti, L., De Martini, P.M., Nappi, R. and Open EMERGEO Working Group, 2018. Surface ruptures following the 30 October 2016 M w 6.5 Norcia earthquake, central Italy. *Journal of Maps*, *14*(2), pp.151-160.

9- Guo, Y., Li, H., Liang, P., Xiong, R., Chaozhong, H. and Xu, Y., 2023. Preliminary report of coseismic surface rupture (part) of Turkey's Mw7. 8 earthquake by remote sensing interpretation. *Earthquake Research Advances*, p.100219.

10- Armijo, R., Pondard, N., Meyer, B., Uçarkus, G., de Lépinay, B.M., Malavieille, J., Dominguez, S., Gustcher, M.A., Schmidt, S., Beck, C. and Cagatay, N., 2005. Submarine fault scarps in the Sea of Marmara pull-apart (North Anatolian Fault): Implications for seismic hazard in Istanbul. *Geochemistry, Geophysics, Geosystems*, *6*(6).

11- Elias, A., Tapponnier, P., Singh, S.C., King, G.C., Briais, A., Daëron, M., Carton, H., Sursock, A., Jacques, E., Jomaa, R. and Klinger, Y., 2007. Active thrusting offshore Mount Lebanon: Source of the tsunamigenic AD 551 Beirut-Tripoli earthquake. *Geology*, *35*(8), pp.755-758.

12- Ueda, H., Kitazato, H. and Jamieson, A., 2023. The submarine fault scarp of the 2011 Tohoku-oki Earthquake in the Japan Trench. *Communications Earth & Environment*, *4*(1), p.476.

13- ten Brink, U., Chaytor, J., Flores, C., Wei, Y., Detmer, S., Lucas, L., Andrews, B. and Georgiopoulou, A., 2023. Seafloor Observations Eliminate a Landslide as the Source of the 1918 Puerto Rico Tsunami. *Bulletin of the Seismological Society of America*, *113*(1), pp.268-280.

14- Escartín, J., Leclerc, F., Olive, J.A., Mevel, C., Cannat, M., Petersen, S., Augustin, N., Feuillet, N., Deplus, C., Bezos, A. and Bonnemains, D., 2016. First direct observation of coseismic slip and seafloor rupture along a submarine normal fault and implications for fault slip history. *Earth and Planetary Science Letters*, *450*, pp.96-107.

15- Hughes, A., Escartín, J., Billant, J., Leclerc, F., Andreani, M., Olive, J.A., Arnaubec, A., Dano, A., Delorme, A., Deplus, C. and Feuillet, N., 2023. Seafloor earthquake ruptures and mass wasting from the 2004 Mw 6.3 Les Saintes submarine earthquake. *Communications Earth & Environment*, *4*(1), p.270.

16- Lee, W.H.K. and E.R. Engdahl (2015). Bibliographical search for reliable seismic moments of large earthquakes during 1900-1979 to compute MW in the ISC-GEM Global Instrumental Reference Earthquake Catalogue (1900-2009), Phys. Earth Planet. Int., 239, 25-32, doi: 10.1016/j.pepi.2014.06.004

17- Brüstle, A., Friederich, W., Meier, T. and Gross, C., 2014. Focal mechanism and depth of the 1956 Amorgos twin earthquakes from waveform matching of analogue seismograms. *Solid Earth*, *5*(2), pp.1027-1044.

18- Konstantinou, K.I., 2010. Crustal rheology of the Santorini–Amorgos zone: Implications for the nucleation depth and rupture extent of the 9 July 1956 Amorgos earthquake, southern Aegean. *Journal of Geodynamics*, *50*(5), pp.400-409.

19- Grigoriadis, V.N., Tziavos, I.N., Tsokas, G.N. and Stampolidis, A., 2016. Gravity data inversion for Moho depth modeling in the Hellenic area. *Pure and Applied Geophysics*, *173*, pp.1223-1241.

20- Papadopoulos, G.A. and Pavlides, S.B., 1992. The large 1956 earthquake in the South Aegean: Macroseismic field configuration, faulting, and neotectonics of Amorgos Island. *Earth and Planetary Science Letters*, *113*(3), pp.383-396.

21- Stiros, S.C., Marangou, L. and Arnold, M., 1994. Quaternary uplift and tilting of Amorgos Island (southern Aegean) and the 1956 earthquake. *Earth and Planetary Science Letters*, *128*(3-4), pp.65-76.

22- Nomikou, P., Hübscher, C., Papanikolaou, D., Farangitakis, G.P., Ruhnau, M. and Lampridou, D., 2018. Expanding extension, subsidence and lateral segmentation within the Santorini-Amorgos basins during Quaternary: Implications for the 1956 Amorgos events, central-south Aegean Sea, Greece. *Tectonophysics*, *722*, pp.138-153.

23- Ambraseys, N.: The seismic sea wave of July 1956 in the Greek Archipelago, J. Geophys. Res., 65, 1257–1265, 1960.

24- Beisel, S., Chubarov, L., Didenkulova, I., Kit, E., Levin, A., Pelinovsky, E., Shokin, Y. and Sladkevich, M., 2009. The 1956 Greek tsunami recorded at Yafo, Israel, and its numerical modeling. *Journal of Geophysical Research: Oceans*, *114*(C9).

25 - Dominey-Howes, D., Cundy, A. and Croudace, I., 2000. High energy marine flood deposits on Astypalaea Island, Greece: possible evidence for the AD 1956 southern Aegean tsunami. *Marine Geology*, *163*(1-4), pp.303-315.

26- Hooft, E.E., Nomikou, P., Toomey, D.R., Lampridou, D., Getz, C., Christopoulou, M.E., O'Hara, D., Arnoux, G.M., Bodmer, M., Gray, M. and Heath, B.A., 2017. Backarc tectonism, volcanism, and mass wasting shape seafloor morphology in the Santorini-Christiana-Amorgos region of the Hellenic Volcanic Arc. *Tectonophysics*, *712*, pp.396-414.

27- Rabinovich, A.B., 1997. Spectral analysis of tsunami waves: Separation of source and topography effects. *Journal of Geophysical Research: Oceans*, *102*(C6), pp.12663-12676.

28 - Andinisari, R., Konstantinou, K.I. and Ranjan, P., 2021. Seismicity along the Santorini-Amorgos zone and its relationship with active tectonics and fluid distribution. *Physics of the Earth and Planetary Interiors*, *312*, p.106660.

29 - Evelpidou, N., Melini, D., Pirazzoli, P. and Vassilopoulos, A., 2012. Evidence of a recent rapid subsidence in the S–E Cyclades (Greece): An effect of the 1956 Amorgos earthquake?. *Continental Shelf Research*, *39*, pp.27-40.

30- Tsampouraki-Kraounaki, K., Sakellariou, D., Rousakis, G., Morfis, I., Panagiotopoulos, I., Livanos, I., Manta, K., Paraschos, F. and Papatheodorou, G., 2021. The Santorini-Amorgos Shear Zone: Evidence for Dextral Transtension in the South Aegean Back-Arc Region, Greece. *Geosciences*, *11*(5), p.216.

31- Preine, J., Hübscher, C., Karstens, J. and Nomikou, P., 2022. Volcano-Tectonic Evolution of the Christiana-Santorini-Kolumbo Rift Zone. *Tectonics*, p.e2022TC007524.

32- Briole, P., Ganas, A., Elias, P. and Dimitrov, D., 2021. The GPS velocity field of the Aegean. New observations, contribution of the earthquakes, crustal blocks model. *Geophysical Journal International*, *226*(1), pp.468-492.

33- Piper, D.J.W. and Perissoratis, C., 2003. Quaternary neotectonics of the South Aegean arc. *Marine Geology*, *198*(3-4), pp.259-288.

34- Feuillet, N., 2013. The 2011–2012 unrest at Santorini rift: Stress interaction between active faulting and volcanism. *Geophysical Research Letters*, *40*(14), pp.3532-3537.

35- Kanamori, H. and Anderson, D.L., 1975. Theoretical basis of some empirical relations in seismology. *Bulletin of the seismological society of America*, *65*(5), pp.1073-1095.

36- Geller, R.J., 1976. Scaling relations for earthquake source parameters and magnitudes. *Bulletin of the Seismological Society of America*, *66*(5), pp.1501-1523.

37- Leclerc F., Escartin J. (2022) AMORGOS-22 cruise, RV L'Europe, https://doi.org/10.17600/18001479

38- Leclerc F., Escartin J. (2023) AMORGOS-23 cruise, RV L'Europe, https://doi.org/10.17600/18003211

39- Benedetti, L., Finkel, R., King, G., Armijo, R., Papanastassiou, D., Ryerson, F.J., Flerit, F., Farber, D. and Stavrakakis, G., 2003. Motion on the Kaparelli fault (Greece) prior to the 1981 earthquake sequence determined from 36Cl cosmogenic dating. *Terra Nova*, *15*(2), pp.118-124.

40- Lyon-Caen, H.E.A., Armijo, R., Drakopoulos, J., Baskoutass, J., Delibassis, N., Gaulon, R., Kouskouna, V., Latoussakis, J., Makropoulos, K., Papadimitriou, P. and Papanastassiou, D., 1988. The 1986 Kalamata (South Peloponnesus) earthquake: Detailed study of a normal fault, evidences for east-west extension in the Hellenic Arc. *Journal of Geophysical Research: Solid Earth*, *93*(B12), pp.14967-15000.

41- Koschinsky, A. and Hein, J.R., 2017. Marine ferromanganese encrustations: archives of changing oceans. *Elements*, *13*(3), pp.177-182.

42- Villani, F., Civico, R., Pucci, S., Pizzimenti, L., Nappi, R. and De Martini, P.M., 2018. A database of the coseismic effects following the 30 October 2016 Norcia earthquake in Central Italy. *Scientific data*, *5*(1), pp.1-11.

43- Armijo, R., Lyon-Caen, H. and Papanastassiou, D., 1991. A possible normal-fault rupture for the 464 BC Sparta earthquake. *Nature*, *351*(6322), pp.137-139.

44- Iezzi, F., Mildon, Z., Walker, J.F., Roberts, G., Goodall, H., Wilkinson, M. and Robertson, J., 2018. Coseismic throw variation across along-strike bends on active normal faults: Implications for displacement versus length scaling of earthquake ruptures. *Journal of Geophysical Research: Solid Earth*, *123*(11), pp.9817-9841.

45- Ambraseys, N., 2009. Earthquakes in the Mediterranean and Middle East: a multidisciplinary study of seismicity up to 1900. *Cambridge University Press.*

46- Papazachos, B.C. and C.B. Papazachou (2003): The earthquakes of Greece 3rd Edition. *Ziti Publ. Thessaloniki, Greece, 286pp. (in Greek).*

47- Albini P., Locati M., Rovida A., Stucchi M. (2013). European Archive of Historical EArthquake Data (AHEAD). *Istituto Nazionale di Geofisica e Vulcanologia (INGV). https://doi.org/10.6092/ingv.it-ahead*

48- Makropoulos, K., Kaviris, G. and Kouskouna, V., 2012. An updated and extended earthquake catalogue for Greece and adjacent areas since 1900. *Natural Hazards and Earth System Sciences*, *12*(5), pp.1425-1430.

49- http://www.geophysics.geol.uoa.gr/frame_en/catal/menucatal_en.html

50- Perrin, C., Manighetti, I., Ampuero, J.P., Cappa, F. and Gaudemer, Y., 2016. Location of largest earthquake slip and fast rupture controlled by along-strike change in fault structural maturity due to fault growth. *Journal of Geophysical Research: Solid Earth*, *121*(5), pp.3666-3685.

51- Hanks, T.C. and Kanamori, H., 1979. A moment magnitude scale. *Journal of Geophysical Research: Solid Earth*, *84*(B5), pp.2348-2350.

52- Wells, D.L. and Coppersmith, K.J., 1994. New empirical relationships among magnitude, rupture length, rupture width, rupture area, and surface displacement. *Bulletin of the seismological Society of America*, *84*(4), pp.974-1002.

53- Sparacino, F., Galuzzi, B.G., Palano, M., Segou, M. and Chiarabba, C., 2022. Seismic coupling for the Aegean-Anatolian region. *Earth-Science Reviews, 228*, p.103993.

54- Georgalas, G. C, 1962. Greece. Catalogue of the Active Volcanoes of the World including solfatara fields. 12, 40, Napoli.

55- Di Giacomo, D., E.R. Engdahl and D.A. Storchak (2018). The ISC-GEM Earthquake Catalogue (1904–2014): status after the Extension Project, Earth Syst. Sci. Data, 10, 1877-1899, doi: 10.5194/essd-10-1877-2018

56- Cordrie, L., Gailler, A., Escartin, J., Feuillet, N. and Heinrich, P., 2020. Simulation of the 2004 tsunami of Les Saintes in Guadeloupe (Lesser Antilles) using new source constraints. *Natural Hazards*, *103*(2), pp.2103-2129.

Methods

Bathymetry data. During the AMORGOS-22[37] and AMORGOS-23[38] cruises, we acquired shallow and deep bathymetry using the multibeam echosounder Kongsberg ME70 onboard R/V Europe. Bathymetry was acquired at low speed (2-5 kt) to densify the beams and thus increase the resolution along the steep fault scarp. During the AMORGOS-22[37] cruise, we also collected near-bottom, high-resolution bathymetry data using the AUV Idef^{x} (IFREMER, France), equipped with a Kongsberg Reson SMF EM2040. The AUV surveyed ~70 m above the seafloor, parallel to the faults. All bathymetric data were processed using GLOBE (IFREMER) and gridded to produce digital elevation models (DEMs) with a 1 m cell size for the AUV and 10 m cell size for the ship bathymetry (Figure 2a).

ROV 3D Digital Outcrop models from video imagery. During the AMORGOS-23[38] cruise, we deployed the HROV Ariane (IFREMER) in order to collect video imagery at multiple locations along the fault scarps (Figure 3, S2). It is equipped with a 4K camera (DeepSea Apex SeaCam) mounted on a pan-and-tilt platform at the front of the vehicle, and a second HD camera mounted on the lower-right corner of the vehicle. We surveyed the fault scarp horizontally and vertically, using overlapping tracks at speeds of <0.5 m/s and at distances of ~2–5 m from outcrops. Extracted video frames (every 2 seconds) were corrected for illumination attenuation prior to processing, using the MATISSE 3D Preprocessing tool[57] (IFREMER). A structure-from-motion technique was then applied with MATISSE 3D software (v.1.4) [57] to obtain three-dimensional digital outcrop models that correspond to vertical transects (method A). The HROV navigation data were used as *a priori* constraints to build the sparse point cloud, and bundle adjustment was performed before densifying the point cloud, meshing and texturing the models. Terrain models are thus georeferenced and scaled to allow geological interpretations and provide proper scaling for quantitative studies with model resolutions of ~1 cm or better.

To verify the obtained displacements with Method A, we used different processing pipelines with two additional methods and algorithms. Method B used the 3DF ZEPHYR software using the HROV navigation data as *a priori* constraints, but without bundle. Method C[58] used the navigation data as *a posteriori* constraint to scale the model. In total, 21 DOMs were obtained that model the seven vertical transects. We used 3DF ZEPHYR's drawing and measuring tools to map the striae, the base and the top of the fresh fault mirror. We measured the minimum and maximum distances on the model that separate the top and bottom of the fault mirror, in the direction of the striae (i.e., along-dip). Figure S2 presents the seven vertical transects modeled with method A. Table S4 presents the measurements for each of the seven sites, measured with the three methods (A, B, C). Overall, the on-fault offset measurements show the same trend. Half of the measurements done with method B and C agrees with measurements performed with method A within 4.8% and 6.4% respectively (i.e. median). A few measurements performed with method C departs by up to 26.5% from method A. The DOM of the vertical transect presented in Figure 3a is very well constrained, as the three methods give similar results (mean on-fault offset of 15.8±0.1). This site displays the largest offset we observed during the dive.

For consistency in the main text and main figures, all on-fault offsets measured and discussed are obtained with MATISSE 3D (method A). Therefore, all vertical offsets and horizontal extensions are derived from method A measurements. Despite this modeling effort, DOMs were misoriented due to inaccurate recording of the pan and tilt of the cameras during acquisition. While this does not impact the on-fault distance measurements, we could not use the DOMs to measure the scarp dip and calculate the vertical offset and horizontal extension discussed in the main text. To overcome this limitation, the 1 m DEM derived from AUV surveys allowed us to measure scarp dip.

Data availability statement

The 1 m DEM from the AMORGOS-22 cruise and the 10 m DEM from the AMORGOS-23 cruise, presented in Figure 2, are available at https://doi.org/10.17882/99212 and https://doi.org/10.17882/90284 respectively.

The HROV-navigation file of dive 1 from the AMORGOS-23 cruise is available at https://campagnes.flotteoceanographique.fr/campagnes/18003211/.

Video-derived 3D Digital Outcrop Models are available at https://doi.org/10.17882/99228

Methods References

57- Arnaubec, A., Ferrera, M., Escartín, J., Matabos, M., Gracias, N. and Opderbecke, J., 2023. Underwater 3D Reconstruction from Video or Still Imagery: Matisse and 3DMetrics Processing and Exploitation Software. *Journal of Marine Science and Engineering*, *11*(5), p.985.

58- Istenič, K.; Gracias, N.; Arnaubec, A.; Escartín, J.; Garcia, R. Scale Accuracy Evaluation of Image-Based 3D Reconstruction Strategies Using Laser Photogrammetry. Remote Sens. 2019, 11, 2093. https://doi.org/10.3390/rs11182093

Acknowledgements: The authors thank the captains and crews of the R/V Europe during the AMORGOS-22 and AMORGOS-23 oceanographic cruises, the AUV and HROV teams of Genavir, and the Flotte Océanographique Française that funded ship time and related expenses. This work has been supported by the French government, through the UCAJEDI Investments in the Future project managed by the National Research Agency (ANR) with the reference number ANR-15-IDEX-01. This work was also supported by the Tellus Program of CNRS-INSU, and by the Observatoire de la Côte d'Azur. We thank the Greek Ministry of Foreign Affairs for the cruise permissions. We thank Christophe Larroque and an anonymous reviewer for their comments on a first version of the manuscript.

Author contributions:

F.L. designed the study, supervised the ship, AUV and ROV data acquisition and processing, processed the 3D models with Matisse 3D and 3DF Zephyr, interpreted the data and wrote the original manuscript. S. P. took part in the ship and ROV data acquisition and bathymetric data processing, interpreted the data and revised the manuscript. N. F. and P. N. took part in the ship, AUV and ROV data acquisition, interpreted the data and revised the manuscript. took part in the ship, AUV and ROV data acquisition, interpreted the data and revised the manuscript. D. L. took part in the ship and AUV data acquisition, processed the ship bathymetric data. P. B. processed the AUV bathymetric data. A. D. supervised and processed the AUV and ship bathymetric data. E. O. processed the 3D models with method C and revised the manuscript. N. G. supervised the 3D model processing and revised the manuscript. J. E. designed the study, interpreted the data and revised the manuscript.

Competing interest declaration:

The authors declare no competing interests.

Additional Information:

Extended data figures (S1 and S2) and tables (S3 and S4) are available for this paper.

Correspondence and requests for materials should be addressed to Frédérique Leclerc (Leclerc@geoazur.unice.fr).

Reply to Reviewers' comments

Large seafloor rupture caused by the 1956 Amorgos tsunamigenic earthquake, Greece

Leclerc* Frédérique, Sylvain Palagonia, Nathalie Feuillet, Paraskevi Nomikou, Danai Lampridou, Paul Barrière, Alexandre Dano, Eduardo Ochoa, Nuno Gracias, Javier Escartin

** Corresponding author : leclerc@geoazur.unice.fr

Reviewer #1 (Remarks to the Author):

This paper reports ROV observation of submarine fault scarp recording movements of a historic tsunami-genic earthquake. The presented data, especially ROV photos (as 3D models), are fascinating and highly suggestive for us about underwater exploration of earthquake faults. Resultant discussions are also clear and reasonable. I thus think it is worth publishing. In some parts, more detailed description is desired to make the story robust. I'll be glad if following my comments help it.

Major comments:
(1) Lines 217-219: Better to describe characteristics of subvertical striae more in detail. For example:
* Striae found on the colluvial wedge surface (Figs. 3a and S-3F) are clearly identified as sediment rills.
* In Fig. S2B, the striae on the mirror are crosscut (covered) by the top of the recent colluvial wedge at their lower end, excluding their origin from current sedimentary processes.

We thank reviewer 1 for this comment. Indeed detailed description were missing and are now included (Line 183- 191). We have re-organize this part of the manuscript, in relation to reviewer #2 comments too, in order to better explain our interpretation of these markers.

* In Fig. S2B, the striae seem to be covered by breccia-like materials labeled as "Block that is part of the colluvial wedge" at their upper ends. However, the wedge seems to consist of finer-grained sediments (white ooze?) as seen in the paleo-wedge in the same fig. and also in the modern wedge in Figs. S1b &c. Therefore, it is more probable that the breccia-like materials are fault breccia hanging on the mirror surface, rather than parts of the colluvial wedge. This interpretation, if correct, supports that the striae are tectoglyphs scratched by the brecciated hanging-wall materials (see the attached file).

We apologize for a mistake on Fig S2b that misled reviewer 1. The label "Block that is part of the colluvial wedge" should not have appeared on this figure. Therefore, as it was a mistake, we removed it and did not address the comment of Reviewer 1.

* In Fig. S2E, striae on the fresh mirror are seemingly covered with remnants of the paleo-wedge. This relation implies that the striae formed not in the last event but in previous events before the paleo-wedge formed (even though the mirror surface appeared in the last event). This also implies that not paleo-wedge sediments but deeper portions of the hanging-wall scratched the mirror surface to form the striation.
No matter whether the authors agree or disagree with arguments above, more detailed description especially on crosscut relations could better constrain the origin and timing of the observed features.

We mentioned the possibility that the striaes are older than the last earthquake in the discussion (line 260).

(2) Each picture in Figs. 3 and S2 is a computed collage of multiple photographs. In each source photograph (or a snapshot of 4K video), brightness might reflect not only color of pictured materials (rock or sediment surfaces), but also lighting: brighter parts are closer to, and darker parts are farther from the ROV LED lights. Such lighting effects seem to be not fully corrected to create 3D collages, resulting in artificially mottled appearance of the presented pictures. This could be a problem for the story: I wonder whether the upper darker parts in Figs. 3 and S2B–G owe really to Mn coating or merely to poor lightning. Because ROV did not go upslope so much (as shown in Fig. 2), the top parts of the observed slopes might have been always remote from the vehicle and thus pictured as dark. One of the ways to cancel this discrepancy may be showing raw pictures for key features. Although 3D models appear attractive, they are not observation (in strict sense) but artificially processed models. I recommend also to show raw pictures as primary data.

During the processing of the 3D models, images are extracted from the videos and corrected from lighting effects, partially compensating for the colour-shift vs.distance artefact cited by the reviewer. Yet, we agree with the reviewer that raw pictures are needed to support our interpretation, that is based on all these optical data and on-board observations during the dives. We thus provide pictures in supplementary materials (Figure S3); raw pictures are already present in the main text (Figure 2). We also provide the video sequence that allowed us to produce the model presented in Figure 2 (Supplementary Movie 1).

(3) Estimation of fault displacement relies on identification of remnants of the last colluvial wedge hanging on the scarp. Therefore, it is better to more clearly describe that there are no other remnants at lower levels than the observed remnants identified as the last. In Fig. S2F, there seems to exist potential another remnant at a lower level than that labeled as paleo-wedge. It is desired to have explanation on what is this. In addition, there might be no proof that remnants of the paleo-wedge are always preserved on the upheaved mirror surface. If the paleo-wedge happened to be unpreserved in a place, the second last could be identified as the last. Such misidentification, if happens, overestimates the fault displacement. Although the authors' identification feels acceptable because all lie at similar levels, I feel it

still better to briefly describe such theoretical limit or assumption before evaluation of displacements.

We agree with reviewer 1 that the remnants of the colluvial wedge is not solely constituted by a thin white line. Instead, at some places and especially in Figure S2d & S2f, the remnants are quite thick and could look like different colluvial wedges, exhumed during different slip events. However, the overall geometry of the remnants does not support this interpretation, as they are piled-up, as sediment strata. The three-quarter profiles of the different DOMs allow to see the different stratas (and we added a new label on the interpretation of the DOM D1_1246, Figure S2f). In Figure S1, described in the main text (line 186-190), we describe the stratas composing the wedge. Thus we interpret the colluvial wedge remnants of Figure 2D and F as a unique piece, made of different stratas (added line 221), linked to a unique exhumation phase. Therefore, we do not discuss the point raised by the reviewer in the paper, as our interpretation is different. However we show and explain our interpretation better (line 221-222).

In addition, the two sites showing such thick remnants also exhibit colors and/or texture (rugosity or presence of gullies) changes above and below the paleo-wedge remnants. These different clues support our interpretation that the paleo-seafloor corresponds to the top of the paleo-wedge, and that we measured the most reasonable offset.

Minor comments:
(4) Better to provide geological background more in detail. What kind of rocks comprise the fault scarp? Are they hard or soft? Even if ROV observation could not specify the exact rock species, citing literature on underwater geology such as dredge reports could be useful. Nature of bed rocks are important for readers to properly understand implication of the observed features.

We than reviewer #1 for this comment that was indeed missing. We re-orgarnised a little bit the paragraphs to add a description (183-193)

(5) Line 180: “At one place”: Better to describe precise location (lat & lon etc.).

Modified into “At the HROV dive site presented below” (line 169)

(6) Line 217 and Fig. 3: The parts indicated as gouge in Fig. 3 looks like covers rather than gouge. The parts are so smooth and fine-grained, whereas gouges usually consist of fractured particles of heterogeneous grain sizes. Because it has passed nearly 70 years, it is natural that the mirror surface is partly blanketed with recent mud. Anyway, it's better to describe the reason why a feature was identified as so.

We thank reviewer for this comment, and added description of the fault gouge (line 200-203). We particularly highlight the fact that this deposit is made of fine-grained material and cm-large clasts, and is indurated, inducing that it is not made of hemipelagic loose sediments. We describe this better, and also added information on Figure 3f. The Supplementary Movie 1 is also provided so that reader can see the gouge clearly.

(7) Is there any published data on ages of ancient tsunami deposits around the study area? If present, they could support the discussion in lines 314–321 on recurrence interval of the tsunami-genic earthquakes.
None exists in the area. A few papers were published on the 1956 Amorgos tsunami deposits, that are cited in this paper, or on tsunamis linked to the Thera eruption of Santorini. Unfortunately, we cannot add this in the discussion.

(8) Fig.2: Although 3D view is somewhat reader-friendly, such a bird's-eye-view cannot show features (slope angle, dimension, etc.) accurately. A plain view topo map, which expresses much more delicate features, has been provided as Fig. S1a. In addition, if topographic cross sections are also shown, readers can more accurately understand the slope characteristics.

Bathymetric profiles were added to Figure S1b and a new figure S2 was created to show how the scarp dip and colluvial wedge slope evolve along the fault strike.

(9) Fig.3: Please clarify whether panels b–e are close-up views of the same 3D model as the panel a or raw pictures.

They are raw figures, it is now clarified in the caption (line 640). A video is also provided so that the reader can visualize the fault plane in addition to the reconstruction (line 648 and Movie 1).

Reviewer #2 (Remarks to the Author):

This is a very well-written and interesting paper that should be of great interest to a wide range of earthquake and tsunami scientists, as well as marine geologists. It describes a study that identifies the source of an import tsunamigenic earthquake in the Mediterranean Sea in 1956. In some cases it is possible to guess with reasonable confidence which submarine fault ruptured to generate a major historic tsunami, there are many cases the source remains enigmatic (like the 1755 Lisbon tsunami). Even for modern tsunamis, the precise mechanism for generation - fault rupture or earthquake-triggered submarine landslide? - is often pootly understood - like the case of the 2018 Paul tsunami. This paper gives what appears to me to be the most compelling case ever for identification of fault rupture that generated a tsunami based on marine geologic evidence. I think its conclusions are supported by the data, and that it represents an important step forward in the study of tsunami sources.
I think that the paper could be published in essentially its present form, although I have a few minor suggested changes as indicated below.

We thank reviewer #2 for his/her positive comments.

1) I was confused by the description of how the “shifted” GPS velocities in Fig. 1 highlight the “stability” of the central Aegean, and wonder if the figure and wording could be improved. There should be a velocity scale for the purple GPS vectors and the reference frame for the velocity determinations should be stated. Are these with respect to the Aegean Sea or the

Eurasian Plate? Which sites do the 15.6 mm/yr east and -25 mm/yr north velocities refer to (obviously both sites have both east and north components), and why do these differ from the 4 mm/yr “relative displacement” (is it not a velocity?, and relative to what?).
In any case velocities which differ from that associated with rigid block motion either reflect deformation do to friction at plate boundaries that experience relative movement, or the presence of additional mcrooplates, or both. I would say they highlight complex tectonics rather than stability.

We have rephrased the caption for simplicity (line 623), and added a scale to the vector of Figure 1.

2) On Line 162, I think it would be worth having a sentence or two to explain what a “fault mirror” is, and what its significance is

Linking this comment to reviewer#1’s comment, we have re-organised the paragraph presenting fault mirror and the different markers of slip (striae and gouge). We first describe our observations, i.e. the striae and gouge. They imply that tectonic movement generated the smooth surface that is thus interpreted to be a fault mirror, a fault surface polished by slip. Line 191-207

Line 56: “hypocenter” -> “hypocentral depth”
Corrected on line 61

Line 97: “entered” -> “inundated”
Corrected on line 84

Line 104: “inducing” -> “so”
Corrected on line 91

Line 116: “archeological masonries” -> “damage to archaeological masonry structures”
Here, the proposition of the reviewer indicates that our phrasing is not adequate to express our thoughts. Therefore, we explain better how archeological masonries were used to gain insights into the causative fault. Line 103-107

Line 263: “is no testimonies”” -> “are no testimonies”
Corrected Line 253

Reviewer #3 (Remarks to the Author):

Dear Authors,

It is with a great interest that I read your manuscript entitled:"The discovery of the large seafloor rupture of the 1956 Amorgos tsunamigenic 1 earthquake (Greece)" co authored by Leclerc F., Palagonia S., Feuillet N., Nomikou P., Lampridou D., Barrière P., Dano A., Ochoa E., Gracias N. and Escartin J.

With your new observations you evidence for the first time a recent seafloor rupture along the active fault of Amorgos (Greece), that may have trigger the tsunami that followed the Amorgos 1956 earthquake, challenging the hypothesis of a landslide as a source for the observed tsunami.
Your study open a new avenue to the study of monitoring large active faults located next to populated area such as islands along subduction zones worldwide. Such systematic studies might allow a better risk assessement and would be benefic for policy makers.
I thus recommend the editor to accept your mansucript with very minor revisions mostly concerning the figures (see my comments in the annotated manuscript).
Best regards

We thank reviewer #3 for his/her positive comments. We have modified the caption of Figure 1 accordingly (lines 619-620), and added orientation to the 3D blocks of Figure 2 and 3.